NLO predictions for t-channel production of single top and fourth generation quarks at hadron colliders

JHEP10(2009)042

(http://iopscience.iop.org/1126-6708/2009/10/042)

Published by IOP Publishing for SISSA

Received: *August 27, 2009*
Accepted: *September 21, 2009*
Published: *October 14, 2009*

NLO predictions for t-channel production of single top and fourth generation quarks at hadron colliders

John M. Campbell,[a] **Rikkert Frederix,**[b,1] **Fabio Maltoni**[c] **and Francesco Tramontano**[d]

[a] *Department of Physics and Astronomy, University of Glasgow, University Avenue, Glasgow G12 8QQ, U.K.*

[b] *PH Department, Theory group, CERN, Route de Meyrin, 1211-CH Geneva, Switzerland*

[c] *Centre for Particle Physics and Phenomenology (CP3), Université catholique de Louvain, Chemin du Cyclotron 2, B-1348 Louvain-la-Neuve, Belgium*

[d] *Università di Napoli Federico II, Dipartimento di Scienze Fisiche and INFN, Sezione di Napoli, Università di Napoli Federico II, via Cintia, I-80126 Napoli, Italy*

E-mail: j.campbell@physics.gla.ac.uk, rikkert.frederix@cern.ch, fabio.maltoni@uclouvain.be, francesco.tramontano@na.infn.it

Abstract: We present updated NLO predictions for the electroweak t-channel production of heavy quarks at the Tevatron and at the LHC. We consider production of single top and fourth generation t' starting from both $2 \to 2$ and $2 \to 3$ Born processes. Predictions for tb' and $t'b'$ cross sections at NLO are also given for the first time. A thorough study of the theoretical uncertainties coming from parton distribution functions, renormalisation and factorisation scale dependence and heavy quark masses is performed.

Keywords: NLO Computations, Heavy Quark Physics, Hadronic Colliders

ArXiv ePrint: 0907.3933

[1] On leave of absence from CP3, Université catholique de Louvain.

doi:10.1088/1126-6708/2009/10/042

JHEP10(2009)042

Contents

JHEP10(2009)042

1 Introduction

The recent observation of electroweak production of single top at the Tevatron [1, 2] has opened a new exciting chapter in top physics. Many other properties of the heaviest of the known quarks are now accessible and will be studied over the coming years at both the Tevatron and the LHC. For instance, single top production has already provided the first direct measurement of $V_{\rm tb}$, i.e. without appealing to unitarity of the CKM matrix.[1] In fact a significant motivation to accurately measure cross sections and distributions for this final state is given by the search for new physics effects [4]. Flavor changing neutral currents, the existence of $W'^{\pm}$, $H^{\pm}$ or of more general four-fermion interactions could be detected as anomalous production of single top. In addition, production of a heavier partner of the top or bottom quarks — associated with a fourth generation $\mathrm{SU}(2)_L$ doublet or a vector-like state — could be of phenomenological relevance [5–8] when produced either in pairs [9–11] or singly [3, 7]. For instance, the presence of a fourth generation is not excluded by precision electroweak and flavor data [3, 12–16], although direct searches at the Tevatron provide some lower bounds on the quark masses. The current 95% confidence level limits are [17],

$$m_{t'} > 256 \text{ GeV}\,, \qquad m_{b'} > 128 \text{ GeV} \tag{1.1}$$

[1] $V_{\rm tb} \gg V_{\rm ts}, V_{\rm td}$, however, has been assumed in the current analyses [1, 2]. Such a constraint could also be lifted with further integrated luminosity [3].

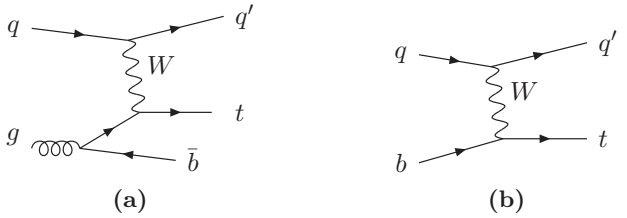

Figure 1. (a) One of two diagrams entering the LO calculation of the $2 \to 3$ single top process; (b) the single LO diagram for the $2 \to 2$ process. The NLO calculations presented in this paper correspond to dressings of these diagrams with additional real and virtual gluon radiation.

with this limit on the b' mass corresponding to a charged current decay. In particular scenarios, where the masses are large and/or there is sizeable mixing with 3rd generation quarks, electroweak production at the LHC can in fact be larger than the usual strong pair production.

In a recent letter [18] we have reported on the first NLO calculation of single-top production in the t channel based on the $2 \to 3$ leading order process, where both heavy quark masses are kept finite (figure 1(a)). This extends previous NLO (QCD or EW) results which are based on the $2 \to 2$ leading order process [19–27]. A comparison of the two calculations allows a first study of their consistency across a broad kinematic range. In this work we perform a thorough analysis of the cross sections for single-top production, for both the $2 \to 2$ (figure 1(b)) and $2 \to 3$ based calculations, including scale dependence and PDF uncertainties, as described in section 2. In section 3 we present results as a function of the top mass, with values as high as 2 TeV in order to provide predictions for a t'. In section 4 we present for the first time the corresponding t-channel cross sections for the production of a top quark in association with a b' and for a 4th generation doublet $t'b'$. In order to illustrate the sensitivity of this channel, we compare these with the NLO predictions for strong pair production. Finally, we conclude with a brief discussion of our results and perspectives for improvement.

2 Methodology

We perform a study similar to that of ref. [28] for the case of $t\bar{t}$ production, presenting our results in the form

$$\sigma = \sigma_{\text{central}} \, {}^{+\Delta\sigma_{\mu+}}_{-\Delta\sigma_{\mu-}} \, {}^{+\Delta\sigma_{\text{PDF}+}}_{-\Delta\sigma_{\text{PDF}-}} , \tag{2.1}$$

where σ_{central} is our best prediction and $\Delta\sigma_{\mu\pm}$ and $\Delta\sigma_{\text{PDF}\pm}$ quantify the uncertainties due to unknown higher orders and our incomplete knowledge of the non-perturbative PDFs, respectively. σ_{central} is tabulated/plotted as a function of the heaviest quark mass, $m_{t^{(\prime)}}$ or $m_{b^{(\prime)}}$. We always quote each source of uncertainty explicitly, except for the plots (figures 2–8) where the total uncertainty band is the direct sum of the two. Our choice of parameters for the best prediction, and the prescription that we have used to evaluate the uncertainties, are specified below.

JHEP10(2009)042

2.1 Best prediction

Our best prediction, σ_{central}, is computed using a similar choice of renormalisation and factorisation scales to what was previously advocated in [18]. For the $2 \to 3$ calculation this corresponds to choosing separate scales on the light and heavy quark lines (μ_l and μ_h respectively), where $\mu_l = (m_t + m_b)/2$ and $\mu_h = (m_t + m_b)/4$. The $2 \to 2$ calculation uses a single overall scale, $m_t/2$, and for both processes the renormalisation and factorisation scales are equal. For a heavy quark with a mass similar to that of the top quark we have shown in ref. [18] that this is a judicious choice of scales. A similar scale choice is also suggested in other processes that feature initial-state gluon splitting into a heavy quark pair, such as $gg \to b\bar{b}H$ [29, 30]. For much larger top quark masses we find similar conclusions, although even smaller scales for the heavy quark line might be preferred. However, for the sake of simplicity, we maintain the same choice since for very high quark masses the accuracy of our calculations will in any case be affected by potentially important threshold resummation effects [31, 32].

We present results for two choices of PDF family, CTEQ6.6 [33] and MSTW2008 [34]. Our central prediction for each of these choices corresponds to the best fit for each family. It is important to note that CTEQ and MSTW use different b masses in their fits ($m_b = 4.5\,\text{GeV}$ and $m_b = 4.75\,\text{GeV}$ respectively). For the results presented here we have used the value prescribed by the PDF set for their respective predictions. In section 3.1 the uncertainty coming from the heavy quark masses is addressed. We note that, since these are 5-flavour PDF sets, we pass to the 4-flavor scheme necessary for a consistent calculation of the tb and $t'b$ processes by including the counterterms of ref. [35]. For tb' and $t'b'$ we always use the pure 5-flavor PDFs.

Though mixings from the CKM matrix are fully included in our calculation, for simplicity we present results with the V_{ij} relative to the third and possibly the fourth generation set to unity, i.e., $V_{\text{tb}} = V_{tb'} = V_{t'b} = V_{t'b'} = 1$ is assumed.

2.2 Uncertainty from higher orders

The uncertainty from uncalculated higher orders in the perturbative expansion is estimated by varying the factorisation and the renormalisation scales μ_{F} and μ_{R} independently around the central scale choice, μ_0. As discussed above, in the $2 \to 3$ calculation we have $\mu_0 = \mu_l$ for the light line and $\mu_0 = \mu_h$ for the heavy line, whereas the $2 \to 2$ calculation uses $\mu_0 = m_t/2$.

The values of μ_F and μ_R that we range over are specified by,

$$(\mu_F, \mu_R) \in \Big\{(2\mu_0, 2\mu_0),\ (2\mu_0, \mu_0),\ (\mu_0, 2\mu_0),\ (\mu_0, \mu_0/2),\ (\mu_0/2, \mu_0),\ (\mu_0/2, \mu_0/2)\Big\}\ . \quad (2.2)$$

In this way we ensure that none of the ratios, μ_F/μ_0, μ_R/μ_0 and μ_F/μ_R, is outside the interval $[\frac{1}{2}, 2]$. These ratios naturally appear as arguments of logarithms at NLO, so restricting them in this way is motivated by the requirement of good perturbative behaviour.

JHEP10(2009)042

The uncertainties are then defined with respect to this set of variations as,

$$\Delta\sigma_{\mu+} = \max_{\{\mu_F,\mu_R\}} \Big[\sigma(\mu_F,\mu_R) - \sigma_{\rm central}\Big]\,, \tag{2.3}$$

$$\Delta\sigma_{\mu-} = -\min_{\{\mu_F,\mu_R\}} \Big[\sigma(\mu_F,\mu_R) - \sigma_{\rm central}\Big]\,. \tag{2.4}$$

2.3 PDF uncertainty

We estimate the PDF uncertainty on our predictions by making use of the additional sets that are supplied by the CTEQ and MSTW collaborations for that purpose. There are 44 such sets for the CTEQ6.6 [33] PDFs and 30 for the MSTW [34] ones, that are organized in pairs (which we call here set_{+i} and set_{-i}). We follow the prescription of MSTW [34] and determine asymmetric uncertainties in the form,

$$\Delta\sigma_{\rm PDF+} = \sqrt{\sum_i \Big(\max\Big[\sigma(set_{+i}) - \sigma(set_0), \sigma(set_{-i}) - \sigma(set_0), 0\Big]\Big)^2}\,, \tag{2.5}$$

$$\Delta\sigma_{\rm PDF-} = \sqrt{\sum_i \Big(\max\Big[\sigma(set_0) - \sigma(set_{+i}), \sigma(set_0) - \sigma(set_{-i}), 0\Big]\Big)^2}\,. \tag{2.6}$$

where all cross sections are evaluated using our central scale choices and the usual (best fit) PDF set is labelled by set_0. This procedure yields an uncertainty at approximately the 90% confidence level.

3 Single top and t' results

We present here the cross sections for single t and t' production, obtained from both the $2 \to 2$ and $2 \to 3$ calculations, as implemented in the Monte Carlo program MCFM [18, 22, 36]. We show results for Run II of the Tevatron and for two LHC energies, 10 TeV and 14 TeV. For single-top production we show results for a number of different values of the top mass around the current best determination [37] and for t' production we investigate quark masses as large as 2 TeV (at the LHC). The dependence on the bottom mass is addressed in a subsection dedicated to the best SM predictions, section 3.1. As mentioned earlier, we remind the reader that in order to make a fair comparison between the $2 \to 2$ and $2 \to 3$ calculations, the bottom mass has to be consistent with the value assumed in the PDFs, i.e., $m_b = 4.5(4.75)$ GeV for the CTEQ6.6 (MSTW2008) PDFs. Here and in the rest of this paper, by 'quark masses' we mean the pole masses that are the input in the modified $\overline{\rm MS}$ renormalisation scheme that we adopted in the calculation of the virtual contributions at NLO. The cross sections and uncertainties are collected in appendix A in tables 2 and 3 (Tevatron), tables 4 and 5 (LHC, 10 TeV) and tables 6 and 7 (LHC, 14 TeV). For each machine, the two tables correspond to our two choices of central PDF. Note that, at the LHC, the rates for production of a heavy top (or t') are different from those of its antiparticle and the two are thus studied separately. The CTEQ6.6 results for the sum of top (or t') and anti-top (or $\bar{t}'$) production are illustrated in figures 2 (Tevatron), 3 (LHC, 10 TeV) and 4 (LHC, 14 TeV), where we also show the NLO rates for the corresponding strong pair production for comparison.

JHEP10(2009)042

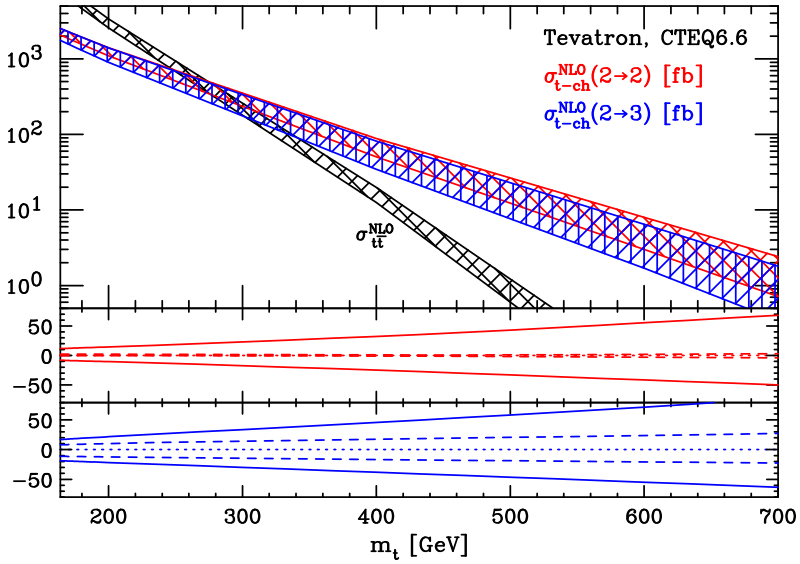

Figure 2. Cross sections (fb) at the Tevatron Run II for the sum of top and anti-top quark production in the t channel, as a function of the top mass obtained with the CTEQ6.6 PDF set and $V_{t^{(\prime)}b} = 1$ in the $2 \to 2$ and $2 \to 3$ schemes. Bands are the total uncertainty (scale+PDF). In the lower plots, dashed is scale uncertainty, solid is scale + PDF. The corresponding data is collected in table 2.

A number of global features are evident from these results. Firstly, the central cross sections predicted by the $2 \to 2$ and $2 \to 3$ processes differ by 5% or less, both at the Tevatron and at the LHC, for masses around the top quark. At the Tevatron, the difference is well within the combined uncertainty from higher orders and PDFs, so we conclude that the two calculations are consistent. At the LHC (10 and 14 TeV) the consistency is marginal, in particular because the uncertainties from the PDFs are (almost) 100% correlated between the two approximations. We stress therefore that in a combined estimate of the total production cross section, the PDF errors should *not* be summed.

For larger masses, i.e. for t' production, the differences are much larger. For a mass of 1 TeV, the $2 \to 2$ prediction using the CTEQ6.6 PDF set is almost twice as large at the Tevatron and 20% bigger at the LHC. However for such large top masses it could well be that the logarithm that is implicitly resummed in the bottom quark distribution function might become relevant or that an even smaller scale choice should be used. Nevertheless we see that the differences between the two calculations can still be accounted for by their uncertainties (with the same PDF caveats as above) and at this stage it is difficult to establish which of the two calculations, the $2 \to 2$ or the $2 \to 3$ one, might be more accurate for the total cross section.

The uncertainty coming from higher orders is estimated to be much larger for the $2 \to 3$ process, particularly at the Tevatron. This is somewhat expected, since the perturbative series for this process begins at $\mathcal{O}(\alpha_s)$ rather than the purely electroweak leading order of the $2 \to 2$ calculation. Our estimate ascribes uncertainties that are typically at the level of a few percent, except for the $2 \to 3$ calculation at the Tevatron where they range from about 10% for the top quark to as large as 30% for a 1 TeV t'.

JHEP10(2009)042

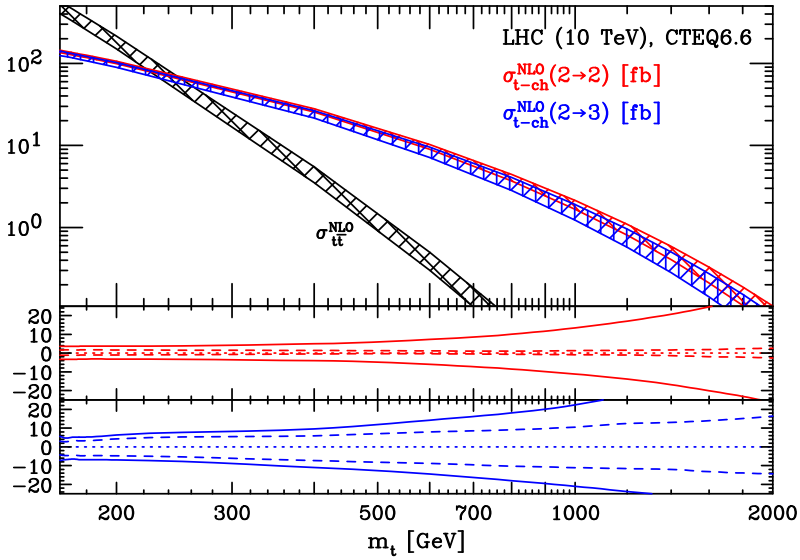

Figure 3. The same as figure 2 but for the LHC 10 TeV. The corresponding data is collected in table 4.

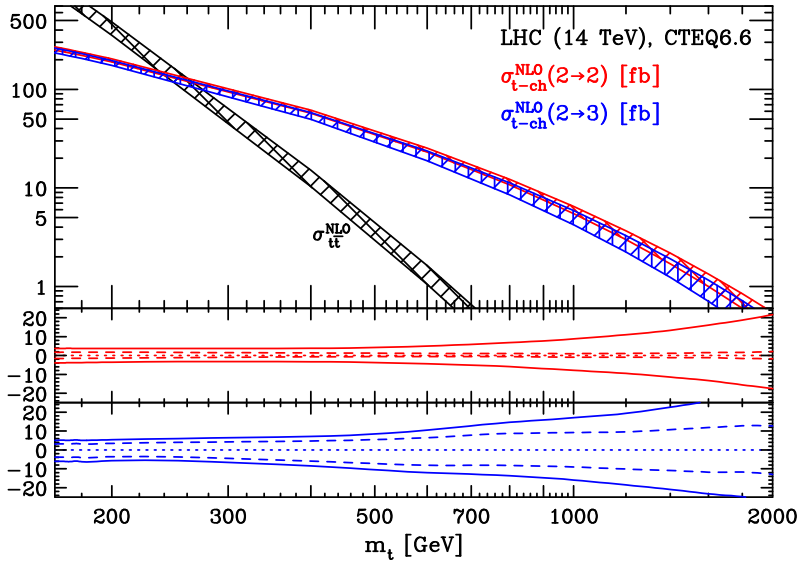

Figure 4. The same as figure 2 but for the LHC 14 TeV. The corresponding data is collected in table 6.

Results from the two different PDF sets are generally in good agreement with one another at NLO. For the top quark, differences are at the level of a couple of percent or less in the $2 \to 2$ calculation, a few percent for the $2 \to 3$ process and are smaller at the LHC than at the Tevatron.

The uncertainty on the cross sections deriving from the PDFs is different between the Tevatron and the LHC. At the Tevatron the PDF uncertainty is particularly large, with the CTEQ6.6 set yielding approximately a 10% uncertainty for the top quark (slightly

JHEP10(2009)042

smaller for MSTW), whilst for a t' it can be considerably larger. This simply represents the limitations of current global PDF determinations, where the gluon distribution at large momentum fractions is not very well constrained by data. This explains not only the much larger percentage uncertainties, but also the greater difference between the CTEQ6.6 and MSTW predictions. For such large masses the cross sections presented here clearly have little phenomenological interest at the Tevatron.

At the LHC the PDF uncertainty on the $2 \to 2$ single top quark cross section is comparable to that coming from the unknown higher orders, whilst it is somewhat smaller for the $2 \to 3$ calculation. For single t' production the two sources of uncertainty are comparable in the $2 \to 3$ case, but the uncertainty from the PDFs clearly dominates for the $2 \to 2$ process.

3.1 Single top cross sections in the SM: bottom and top mass dependence

For the case of single top production in the Standard Model, whose cross section can be predicted quite accurately, it is important to investigate in detail its dependence on both heavy quark masses. In the following we discuss the bottom and top mass effects independently, having checked explicitly that this is a very good approximation.

To our knowledge the bottom quark mass dependence of the total single top cross section has never been addressed in detail. There are two different ways in which the bottom mass can enter the final results, i.e., through logarithmic and power correction terms. In the $2 \to 3$ calculation both effects explicitly depend on the pole mass parameter that is already present at LO in the matrix element (and in the phase space boundaries). In the $2 \to 3$ based computation it is therefore trivial to quantify the bottom mass dependence. On the other hand, disentangling the relative impact of the logarithmic terms from those that are power suppressed requires some analytical work. In the $2 \to 2$ calculation the situation is reversed. The two sources are separated from the start: the effect of the logarithms is resummed in the bottom PDF while the power-like terms at NLO come from the (subtracted) real correction diagrams $qg \to tbq'$. The effect of the b mass from the latter source has already been studied, see for instance ref. [38], and found to be very small. We have checked that changing the bottom mass from $\sim$5 GeV to zero results in a difference below 0.5%. However the logarithmic corrections, which have so far been neglected, are quite sizeable. In the $2 \to 2$ calculation the logarithmic dependence on the bottom quark mass is "hidden" in the starting condition for the evolution of the b-PDF. To study its impact we have generated various sets of PDFs for different bottom masses in the range $4\,\text{GeV} < m_b < 5\,\text{GeV}$, using the evolution code provided by the CTEQ collaboration. As a result we find that the $2 \to 2$ cross sections on average decrease by about 1.2%, 0.86%, 0.80% per 100 MeV increase of m_b at the Tevatron, LHC at 10 TeV and 14 TeV, respectively. Such a dependence is fully reproduced by the $2 \to 3$ calculation which gives similar (corresponding) results, namely 1.0%, 0.83% and 0.76%. We conclude that the b mass dependence should be included as a source of uncertainty in the final predictions for the SM total cross sections.

As far as the top quark mass dependence is concerned, this can be studied easily in both the $2 \to 2$ and $2 \to 3$ calculations. Here we provide formulae that can be used to

JHEP10(2009)042

Collider		Born	MSTW2008			CTEQ6.6		
			σ_0	A	B	σ_0	A	B
Tevatron	$t=\bar{t}$	$2\to 2$	$994^{+24\ +61}_{-2\ -52}$	-3.01	5.2	$981^{+23\ +98}_{-3\ -82}$	-2.97	5.0
		$2\to 3$	$942^{+86\ +53}_{-113\ -43}$	-3.11	4.9	$935^{+82\ +88}_{-107\ -74}$	-3.08	5.3
LHC (10 TeV)	t	$2\to 2$	$84.4^{+1.4\ +1.1}_{-1.0\ -1.0}$	-1.48	1.1	$83.5^{+1.4\ +1.5}_{-1.1\ -1.7}$	-1.50	1.0
		$2\to 3$	$80.3^{+3.2\ +1.1}_{-3.7\ -1.0}$	-1.60	2.2	$79.8^{+2.9\ +1.4}_{-3.4\ -1.6}$	-1.54	3.3
	$\bar{t}$	$2\to 2$	$48.3^{+0.8\ +0.7}_{-0.5\ -1.0}$	-1.57	1.7	$46.6^{+0.8\ +1.0}_{-0.5\ -1.1}$	-1.58	1.2
		$2\to 3$	$45.4^{+1.7\ +0.7}_{-2.1\ -1.0}$	-1.54	0.4	$44.2^{+1.2\ +1.0}_{-2.0\ -1.1}$	-1.68	0.9
LHC (14 TeV)	t	$2\to 2$	$154.3^{+2.9\ +2.2}_{-2.5\ -2.2}$	-1.32	1.1	$152.9^{+3.0\ +3.0}_{-2.3\ -3.4}$	-1.35	2.2
		$2\to 3$	$146.8^{+4.3\ +2.2}_{-5.0\ -2.1}$	-1.40	4.6	$147.0^{+5.0\ +2.7}_{-5.7\ -3.1}$	-1.35	0.9
	$\bar{t}$	$2\to 2$	$94.2^{+1.6\ +1.2}_{-1.5\ -1.9}$	-1.42	1.1	$91.1^{+1.5\ +1.8}_{-1.5\ -2.1}$	-1.42	0.7
		$2\to 3$	$88.7^{+2.6\ +1.3}_{-3.0\ -1.8}$	-1.49	3.1	$86.8^{+2.4\ +1.8}_{-3.7\ -2.0}$	-1.46	0.9

Table 1. Parameters to interpolate the cross section (in fb for the Tevatron, pb for the LHC) and the corresponding uncertainties for top quark masses around the default value of $\sigma_0 = \sigma(m_t = 172\text{ GeV})$.

obtain the cross section and the corresponding uncertainties for any top quark mass in the range $164\,\text{GeV} < m_t < 180\,\text{GeV}$, to an accuracy better than 1%. We fit the mass dependence of the cross section using a quadric centered on $\sigma_0 = \sigma(m_t = 172\text{ GeV})$,

$$\sigma(m_t) = \sigma_0 \left[1 + \left(\frac{m_t - 172}{172} \right) A + \left(\frac{m_t - 172}{172} \right)^2 B \right], \tag{3.1}$$

where m_t is measured in GeV. The (dimensionless) coefficients A and B for both the $2 \to 2$ and $2 \to 3$ processes are given in table 1.

4 tb' and $t'b'$ results

Production of a b', together with either a top quark or an additional t', can be computed at NLO accuracy starting from the $2 \to 3$ Standard Model single-top process. Since the final state contains two heavy particles, the expected rates are probably out of the reach of the sensitivity of the Tevatron and early LHC running. Therefore we present results for the 14 TeV LHC energy only, but explore a range of different t' and b' masses.

For $b'\bar{t}$ (and $\bar{b}'t$) production the cross sections and their uncertainties are tabulated for both choices of PDF set in tables 8 and 9, collected in appendix B. The two sources of uncertainty considered here are of a comparable size, leading to an overall accuracy running from a few percent for $m_{b'} = 200\,\text{GeV}$ up to about 30% for the highest masses considered, once again due to the PDF uncertainty in that kinematic region. The cross sections for the sum of $b'\bar{t}$ and $\bar{b}'t$ production including uncertainties are also plotted in figure 5 for the CTEQ6.6 PDF set. For comparison strong production of b' pairs is also shown.

JHEP10(2009)042

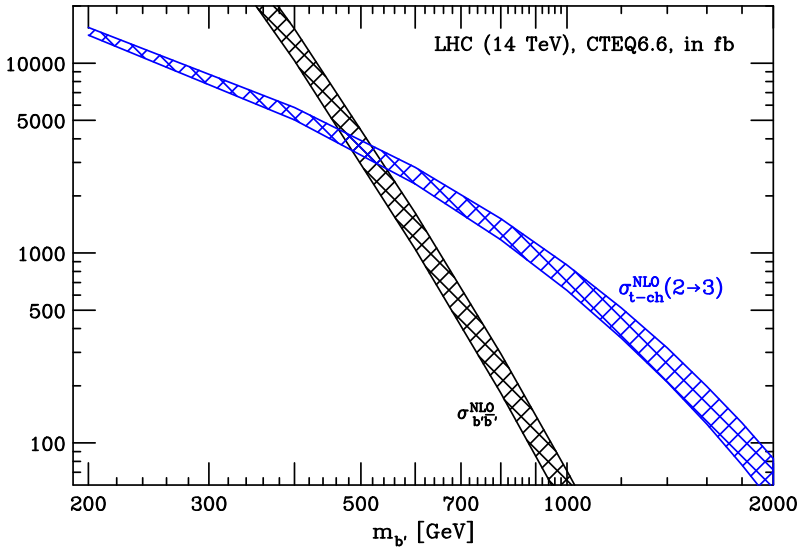

Figure 5. Cross sections (fb) at the LHC 14 TeV for $b'\bar{t}$ plus $\bar{b}'t$ production as a function of $m_{b'}$ obtained with the CTEQ6.6 PDF set and $V_{tb'} = 1$. Bands are the total uncertainty (scale+PDF).The corresponding data is collected in table 8.

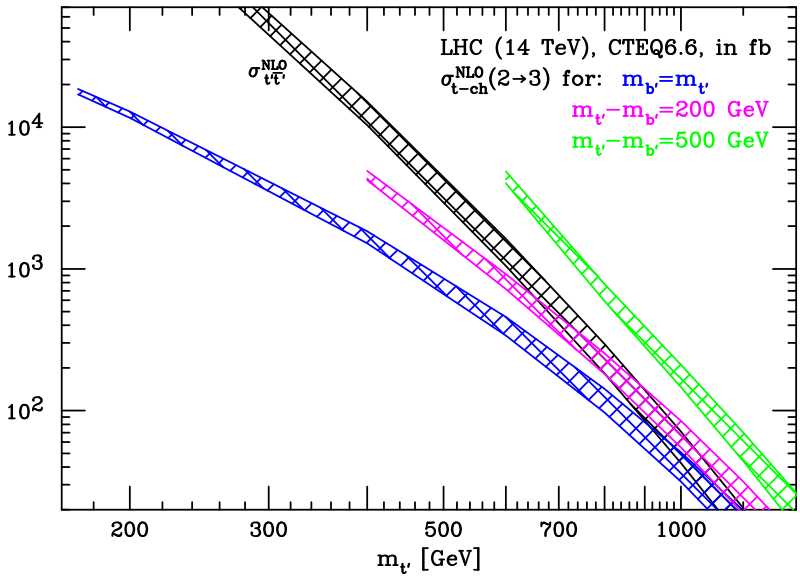

Figure 6. Cross sections (fb) at the LHC 14 TeV for $t'\bar{b}'$ plus $\bar{t}'b'$ production as a function of $m_{t\prime}$ obtained with the CTEQ6.6 PDF set and $V_{t'b'} = 1$. Bands are the total uncertainty (scale+PDF). The corresponding data is collected in table 10.

In the case of $t'b'$ production we consider five different scenarios: $m_{b'} = m_{t'}$, $m_{t'} - m_{b'} = 200\,\text{GeV}$ and $m_{t'} - m_{b'} = 500\,\text{GeV}$ as a function of the t' mass and $m_{b'} - m_{t'} = 200\,\text{GeV}$ and $m_{b'} - m_{t'} = 500\,\text{GeV}$ as a function of the b' mass. Note that mass splittings of this magnitude in a fourth generation would induce a shift in the ρ parameter incompatible with precision EW measurements [39]. However, as our purpose is to provide benchmark

JHEP10(2009)042

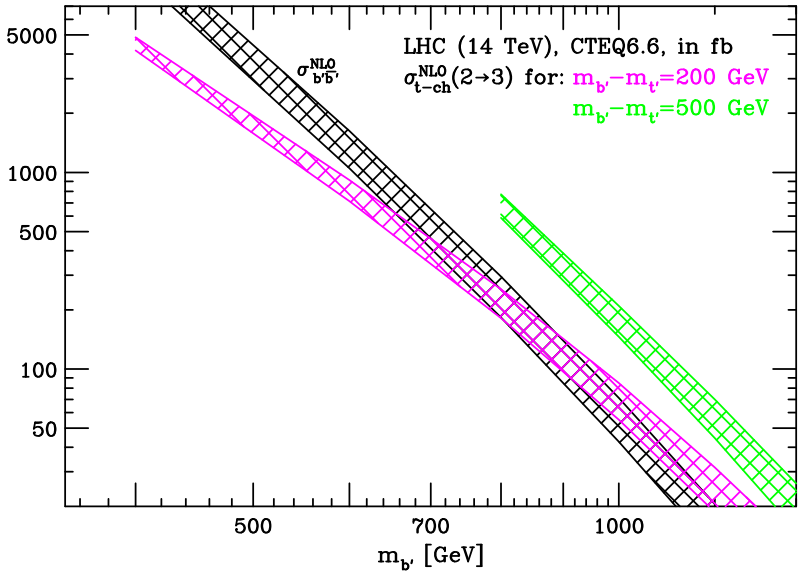

Figure 7. Cross sections (fb) at the LHC 14 TeV for $b'\bar{t}'$ plus $\bar{b}'t'$ production as a function of $m_{b'}$ obtained with the CTEQ6.6 PDF set and $V_{t'b'} = 1$. Bands are the total uncertainty (scale+PDF). The corresponding data is collected in able 12.

cross-sections useful for constructing new models we neglect such constraints here. For instance, introducing extra matter could compensate for these effects and/or the b' and t' might be higher representations of the $SU(2)_L$ symmetry group (with the only constraint being the one unit of charge between two quarks).

The cross sections and uncertainties in the five scenarios are also tabulated in the appendices, for the first three cases together in tables 10 and 11 and for the latter two together in tables 12 and 13, using the CTEQ6.6 and MSTW2008 PDF sets respectively. The CTEQ6.6 results for the first three scenarios are illustrated in figure 6 as the sum of $t'\bar{b}'$ and $\bar{t}'b'$ production, where we also show the NLO rates for $t'\bar{t}'$ for comparison. The latter two scenarios are plotted in figure 7 together with the NLO $b'\bar{b}'$ cross sections and uncertainties for comparison.

We conclude this section by briefly commenting on the symmetry properties of the results for the cross sections. $\mathcal{CP}$ invariance implies that simultaneously interchanging the t' and b' masses, together with the chirality of the Wtb vertex from left- to right-handed, gives the same cross section. By performing either a $\mathcal{C}$ or $\mathcal{P}$ transformation individually, one can pass from the case with $m_{t'} - m_{b'} = 200(500)$ GeV to the case with $m_{b'} - m_{t'} = 200(500)$ GeV, and vice-versa. It is interesting to note that the above cases, while not related by a symmetry, lead to similar total rates. The differences arise from angular dependences in the matrix elements that are proportional to β, the velocity of the heavy quarks. Since these terms are integrated over the available phase space and they are themselves small for high heavy quark masses, they result in only minor differences.

JHEP10(2009)042

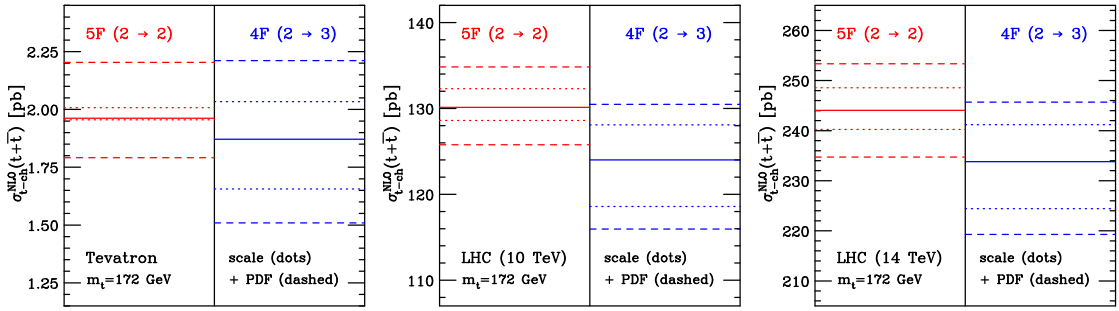

Figure 8. Total cross section at NLO for the $2 \to 2$ and $2 \to 3$ at the Tevatron (top), LHC 10 TeV (bottom-left) and LHC 14 TeV (bottom-right).

5 Conclusions

The recent discovery of single top production at the Tevatron opens the door to more extensive studies of this final state both there and at the LHC. In this paper we have presented an up-to-date and systematic study of both the cross sections that should be expected in this channel and their associated theoretical uncertainties. Cross sections have been computed at NLO accuracy in the strong coupling, starting from two Born approximations corresponding to $2 \to 2$ and $2 \to 3$ scattering processes. Our best predictions for t-channel single top cross sections in the $2 \to 2$ and $2 \to 3$ schemes, with $m_t = 172 \pm 1.7\,\text{GeV}$, $m_b = 4.5 \pm 0.2\,\text{GeV}$ and computed using the CTEQ6.6 PDF set, are:

$\sigma^{\text{NLO}}_{\text{t-ch}}(t+\bar{t})$	$2 \to 2$ (pb)				$2 \to 3$ (pb)			
Tevatron Run II	$1.96\ ^{+0.05}_{-0.01}$	$^{+0.20}_{-0.16}$	$^{+0.06}_{-0.06}$	$^{+0.05}_{-0.05}$	$1.87\ ^{+0.16}_{-0.21}$	$^{+0.18}_{-0.15}$	$^{+0.06}_{-0.06}$	$^{+0.04}_{-0.04}$
LHC (10 TeV)	$130\ ^{+2}_{-2}$	$^{+3}_{-3}$	$^{+2}_{-2}$	$^{+2}_{-2}$	$124\ ^{+4}_{-5}$	$^{+2}_{-3}$	$^{+2}_{-2}$	$^{+2}_{-2}$
LHC (14 TeV)	$244\ ^{+5}_{-4}$	$^{+5}_{-6}$	$^{+3}_{-3}$	$^{+4}_{-4}$	$234\ ^{+7}_{-9}$	$^{+5}_{-5}$	$^{+3}_{-3}$	$^{+4}_{-4}$

The first two uncertainties are computed according to the procedure outlined in section 2 and we have used CTEQ6.6 in order to provide the most conservative predictions. These results are also depicted in the plots of figure 8. The third and fourth uncertainties are related to the top mass and bottom mass uncertainties, respectively.

As the results in the two schemes are in substantial agreement and a priori provide equally accurate though different theoretical descriptions of the same process, one could try to combine them. We think that this is a legitimate approach (once correlations among the theoretical errors, scale and PDF, are taken into account), however, we prefer to present the predictions separately.

In addition, we have also presented cross sections for the production of a fourth generation b', both in association with a top quark and with its partner t'. These cross sections set useful benchmarks for future searches, particularly at the LHC where very heavy quarks with sizeable mixing with third generation quarks or very large mass splittings would be preferentially produced from t-channel production rather than in pairs via the strong interaction.

Although the cross sections presented here embody the current state-of-the-art, a number of avenues for future refinement are evident. First, given the importance of threshold

JHEP10(2009)042

resummation in both the s-channel and pair production modes, the t-channel predictions here could be further improved by including such effects. This would be particularly important at the Tevatron and for high mass t' production at the LHC. Second, in the near future a calculation of the $2 \to 2$ process at NNLO should be feasible. With such a calculation one would be able to better assess the importance of higher order effects in the strong coupling as well as the resummation of collinear logarithms in the bottom quark PDF. This could help to confirm whether these logarithms are large enough that their resummation leads to an important effect, which does not appear to be the case given the reasonable agreement between the $2 \to 2$ and $2 \to 3$ NLO calculations presented here.

Acknowledgments

We are grateful to Fred Olness for providing us with the means to generate PDFs for different bottom quark masses and to Pavel Demin and the IT staff of CP3 for the computing support.

JHEP10(2009)042

A Cross sections and uncertainties for single top and t' production

top mass (GeV)	$2 \to 2$ (fb)	$2 \to 3$ (fb)
164	(1059) $1127^{+27\ +106}_{-2\ -89}$	(790) $1080^{+88\ +96}_{-121\ -80}$
168	(985) $1052^{+23\ +102}_{-3\ -86}$	(729) $1006^{+83\ +93}_{-115\ -77}$
172	(917) $981^{+23\ +98}_{-3\ -82}$	(672) $935^{+82\ +88}_{-107\ -74}$
176	(854) $916^{+21\ +95}_{-2\ -79}$	(621) $872^{+76\ +85}_{-101\ -71}$
180	(796) $856^{+20\ +91}_{-3\ -76}$	(575) $812^{+74\ +82}_{-95\ -68}$
200	(561) $613^{+13\ +75}_{-2\ -62}$	(391) $575^{+58\ +66}_{-71\ -54}$
400	(23.7) $33.5^{+0.4\ +10.4}_{-0.3\ -8.0}$	(13.1) $27.9^{+4.9\ +7.9}_{-4.7\ -6.0}$
600	(1.24) $2.57^{+0.05\ +1.38}_{-0.07\ -0.99}$	(0.59) $1.88^{+0.45\ +0.90}_{-0.39\ -0.64}$
800	(0.064) $0.202^{+0.009\ +0.155}_{-0.010\ -0.107}$	(0.026) $0.126^{+0.039\ +0.088}_{-0.031\ -0.060}$
1000	(0.003) $0.013^{+0.001\ +0.013}_{-0.001\ -0.008}$	(0.001) $0.007^{+0.002\ +0.006}_{-0.002\ -0.004}$

Table 2. NLO cross sections (fb) at the Tevatron Run II for top quark production in the t channel, as a function of the top mass obtained with the CTEQ6.6 PDF set and $V_{t^{(\prime)}b} = 1$. In the second (third) column the $2 \to 2$ ($2 \to 3$) results are shown, where the first uncertainty comes from renormalisation and factorisation scales variation and the second from PDF errors. Numbers in parenthesis refer to the corresponding LO results. Cross sections for anti-top are the same and are not displayed. These results are plotted in figure 2 where the scale and PDF uncertainties are combined linearly.

top mass (GeV)	$2 \to 2$ (fb)	$2 \to 3$ (fb)
164	(1211) $1145^{+28\ +66}_{-2\ -57}$	(893) $1089^{+94\ +58}_{-127\ -47}$
168	(1131) $1067^{+27\ +63}_{-2\ -54}$	(827) $1013^{+88\ +56}_{-122\ -45}$
172	(1056) $994^{+24\ +61}_{-2\ -52}$	(764) $942^{+86\ +53}_{-113\ -43}$
176	(987) $928^{+23\ +58}_{-3\ -50}$	(707) $876^{+80\ +51}_{-107\ -41}$
180	(922) $866^{+21\ +56}_{-3\ -47}$	(655) $816^{+75\ +49}_{-100\ -39}$
200	(661) $618^{+14\ +45}_{-3\ -38}$	(450) $574^{+61\ +39}_{-74\ -31}$
400	(33.0) $30.0^{+0.4\ +5.1}_{-0.3\ -4.0}$	(16.6) $24.9^{+4.7\ +3.7}_{-4.4\ -2.8}$
600	(2.032) $1.811^{+0.040\ +0.512}_{-0.060\ -0.389}$	(0.813) $1.352^{+0.342\ +0.323}_{-0.290\ -0.235}$
800	(0.116) $0.100^{+0.005\ +0.042}_{-0.005\ -0.030}$	(0.038) $0.067^{+0.022\ +0.023}_{-0.016\ -0.016}$
1000	(0.005) $0.004^{+0.001\ +0.002}_{-0.000\ -0.002}$	(0.001) $0.003^{+0.000\ +0.001}_{-0.001\ -0.001}$

Table 3. Same as table 2 but for the MSTW2008 PDF set.

JHEP10(2009)042

top mass (GeV)		$2 \to 2$ (pb)	$2 \to 3$ (pb)
164	t	$(80.9)\ 89.5^{+1.5\ +1.7}_{-1.1\ -1.8}$	$(80.9)\ 86.0^{+2.6\ +1.6}_{-3.8\ -1.7}$
	$\bar{t}$	$(44.1)\ 50.2^{+0.8\ +1.1}_{-0.5\ -1.2}$	$(43.3)\ 47.7^{+1.4\ +1.9}_{-2.0\ -2.2}$
168	t	$(78.2)\ 86.4^{+1.6\ +1.6}_{-1.0\ -1.8}$	$(77.7)\ 83.0^{+2.4\ +1.5}_{-3.9\ -1.6}$
	$\bar{t}$	$(42.6)\ 48.4^{+0.7\ +1.0}_{-0.6\ -1.2}$	$(41.6)\ 46.0^{+1.2\ +1.0}_{-2.1\ -1.1}$
172	t	$(75.6)\ 83.5^{+1.4\ +1.5}_{-1.1\ -1.7}$	$(74.8)\ 79.8^{+2.9\ +1.4}_{-3.4\ -1.6}$
	$\bar{t}$	$(41.1)\ 46.6^{+0.8\ +1.0}_{-0.5\ -1.1}$	$(39.8)\ 44.2^{+1.2\ +1.0}_{-2.0\ -1.1}$
176	t	$(73.1)\ 80.6^{+1.4\ +1.5}_{-0.9\ -1.6}$	$(71.9)\ 77.2^{+2.6\ +1.4}_{-3.8\ -1.5}$
	$\bar{t}$	$(39.7)\ 44.9^{+0.7\ +1.0}_{-0.5\ -1.1}$	$(38.3)\ 42.4^{+1.3\ +0.9}_{-1.9\ -1.1}$
180	t	$(70.8)\ 77.9^{+1.3\ +1.4}_{-0.8\ -1.6}$	$(68.8)\ 74.6^{+2.3\ +1.4}_{-3.7\ -1.4}$
	$\bar{t}$	$(38.3)\ 43.3^{+0.8\ +0.9}_{-0.4\ -1.1}$	$(36.6)\ 40.9^{+1.5\ +0.9}_{-1.8\ -1.0}$
200	t	$(60.1)\ 66.1^{+1.1\ +1.2}_{-0.7\ -1.3}$	$(57.1)\ 62.6^{+2.6\ +1.2}_{-3.1\ -1.2}$
	$\bar{t}$	$(32.3)\ 36.4^{+0.6\ +0.8}_{-0.3\ -0.9}$	$(30.0)\ 33.8^{+1.5\ +0.8}_{-1.4\ -0.9}$
400	t	$(15.86)\ 17.65^{+0.24\ +0.53}_{-0.08\ -0.52}$	$(12.65)\ 16.13^{+0.93\ +0.49}_{-1.21\ -0.47}$
	$\bar{t}$	$(7.87)\ 8.99^{+0.13\ +0.41}_{-0.04\ -0.43}$	$(6.13)\ 8.01^{+0.50\ +0.39}_{-0.56\ -0.40}$
600	t	$(5.65)\ 6.46^{+0.07\ +0.35}_{-0.03\ -0.31}$	$(4.09)\ 5.68^{+0.46\ +0.31}_{-0.50\ -0.27}$
	$\bar{t}$	$(2.62)\ 3.10^{+0.04\ +0.23}_{-0.01\ -0.23}$	$(1.84)\ 2.66^{+0.20\ +0.21}_{-0.24\ -0.20}$
800	t	$(2.35)\ 2.77^{+0.03\ +0.23}_{-0.02\ -0.19}$	$(1.58)\ 2.39^{+0.22\ +0.19}_{-0.25\ -0.16}$
	$\bar{t}$	$(1.025)\ 1.263^{+0.012\ +0.138}_{-0.009\ -0.127}$	$(0.672)\ 1.053^{+0.093\ +0.116}_{-0.104\ -0.106}$
1000	t	$(1.071)\ 1.311^{+0.019\ +0.146}_{-0.012\ -0.121}$	$(0.680)\ 1.093^{+0.121\ +0.118}_{-0.121\ -0.096}$
	$\bar{t}$	$(0.442)\ 0.570^{+0.006\ +0.082}_{-0.005\ -0.073}$	$(0.274)\ 0.462^{+0.043\ +0.066}_{-0.051\ -0.059}$
1200	t	$(0.518)\ 0.660^{+0.010\ +0.095}_{-0.006\ -0.077}$	$(0.315)\ 0.537^{+0.068\ +0.073}_{-0.062\ -0.059}$
	$\bar{t}$	$(0.203)\ 0.275^{+0.004\ +0.050}_{-0.003\ -0.043}$	$(0.120)\ 0.217^{+0.026\ +0.038}_{-0.026\ -0.033}$
1400	t	$(0.262)\ 0.348^{+0.006\ +0.062}_{-0.005\ -0.049}$	$(0.153)\ 0.276^{+0.037\ +0.045}_{-0.033\ -0.036}$
	$\bar{t}$	$(0.097)\ 0.140^{+0.002\ +0.031}_{-0.002\ -0.026}$	$(0.056)\ 0.108^{+0.013\ +0.023}_{-0.013\ -0.019}$
1600	t	$(0.136)\ 0.190^{+0.004\ +0.041}_{-0.004\ -0.032}$	$(0.077)\ 0.148^{+0.021\ +0.029}_{-0.020\ -0.022}$
	$\bar{t}$	$(0.048)\ 0.074^{+0.001\ +0.019}_{-0.001\ -0.016}$	$(0.027)\ 0.055^{+0.008\ +0.014}_{-0.007\ -0.011}$
1800	t	$(0.072)\ 0.107^{+0.003\ +0.027}_{-0.002\ -0.021}$	$(0.040)\ 0.081^{+0.012\ +0.018}_{-0.011\ -0.014}$
	$\bar{t}$	$(0.025)\ 0.040^{+0.001\ +0.012}_{-0.001\ -0.010}$	$(0.013)\ 0.029^{+0.004\ +0.008}_{-0.004\ -0.007}$
2000	t	$(0.039)\ 0.061^{+0.002\ +0.018}_{-0.002\ -0.014}$	$(0.021)\ 0.045^{+0.007\ +0.012}_{-0.006\ -0.009}$
	$\bar{t}$	$(0.013)\ 0.022^{+0.001\ +0.008}_{-0.001\ -0.006}$	$(0.007)\ 0.016^{+0.003\ +0.005}_{-0.002\ -0.004}$

Table 4. NLO cross sections (pb) at the LHC 10 TeV for top and anti-top quarks production, as a function of the top mass obtained with the CTEQ6.6 PDF set and $V_{t^{(\prime)}b} = 1$. In the second (third) column the $2 \to 2$ ($2 \to 3$) results are shown, where the first uncertainty comes from renormalisation and factorisation scales variation and the second from PDF errors. Numbers in parenthesis refer to the corresponding LO results. These results are plotted in figure 3 where the scale and PDF uncertainties are combined linearly.

JHEP10(2009)042

top mass (GeV)		$2 \to 2$ (pb)	$2 \to 3$ (pb)
164	t	(82.0) $90.4^{+1.6\ +1.2}_{-1.1\ -1.1}$	(82.3) $86.7^{+2.6\ +1.2}_{-4.0\ -1.0}$
	$\bar{t}$	(46.4) $52.1^{+0.9\ +0.8}_{-0.6\ -1.1}$	(45.8) $48.7^{+1.8\ +0.7}_{-1.8\ -1.0}$
168	t	(79.2) $87.3^{+1.6\ +1.1}_{-1.1\ -1.1}$	(79.1) $83.5^{+2.7\ +1.2}_{-4.0\ -1.0}$
	$\bar{t}$	(44.7) $50.2^{+0.9\ +0.8}_{-0.6\ -1.0}$	(43.8) $47.3^{+1.1\ +0.8}_{-2.2\ -1.0}$
172	t	(76.6) $84.4^{+1.4\ +1.1}_{-1.0\ -1.0}$	(76.0) $80.3^{+3.2\ +1.1}_{-3.7\ -0.9}$
	$\bar{t}$	(43.2) $48.3^{+0.8\ +0.7}_{-0.5\ -1.0}$	(42.0) $45.4^{+1.7\ +0.7}_{-2.1\ -0.9}$
176	t	(74.1) $81.6^{+1.4\ +1.1}_{-0.9\ -1.0}$	(73.1) $77.6^{+2.3\ +1.1}_{-3.4\ -0.9}$
	$\bar{t}$	(41.7) $46.6^{+0.8\ +0.7}_{-0.5\ -1.0}$	(40.3) $43.7^{+1.2\ +0.7}_{-1.9\ -0.9}$
180	t	(71.7) $78.8^{+1.4\ +1.0}_{-0.8\ -0.9}$	(70.3) $74.6^{+3.0\ +1.0}_{-3.2\ -0.9}$
	$\bar{t}$	(40.3) $45.0^{+0.7\ +0.7}_{-0.5\ -0.9}$	(38.6) $42.3^{+1.0\ +0.7}_{-2.2\ -0.9}$
200	t	(61.1) $67.0^{+1.1\ +0.9}_{-0.6\ -0.8}$	(58.2) $63.3^{+2.6\ +0.9}_{-3.2\ -0.7}$
	$\bar{t}$	(34.1) $37.8^{+0.6\ +0.6}_{-0.4\ -0.8}$	(31.7) $35.3^{+0.9\ +0.6}_{-1.7\ -0.8}$
400	t	(16.43) $18.02^{+0.22\ +0.38}_{-0.10\ -0.30}$	(13.02) $16.37^{+0.98\ +0.35}_{-1.31\ -0.26}$
	$\bar{t}$	(8.51) $9.33^{+0.13\ +0.29}_{-0.06\ -0.32}$	(6.55) $8.33^{+0.45\ +0.26}_{-0.65\ -0.28}$
600	t	(6.01) $6.60^{+0.08\ +0.23}_{-0.03\ -0.19}$	(4.27) $5.78^{+0.48\ +0.20}_{-0.53\ -0.15}$
	$\bar{t}$	(2.90) $3.19^{+0.04\ +0.15}_{-0.02\ -0.16}$	(1.99) $2.74^{+0.21\ +0.16}_{-0.26\ -0.16}$
800	t	(2.57) $2.82^{+0.03\ +0.14}_{-0.02\ -0.11}$	(1.68) $2.40^{+0.24\ +0.12}_{-0.25\ -0.09}$
	$\bar{t}$	(1.167) $1.281^{+0.012\ +0.084}_{-0.010\ -0.082}$	(0.734) $1.064^{+0.092\ +0.068}_{-0.114\ -0.064}$
1000	t	(1.207) $1.324^{+0.015\ +0.088}_{-0.014\ -0.070}$	(0.733) $1.091^{+0.127\ +0.069}_{-0.124\ -0.050}$
	$\bar{t}$	(0.516) $0.568^{+0.007\ +0.048}_{-0.005\ -0.045}$	(0.303) $0.453^{+0.052\ +0.037}_{-0.051\ -0.033}$
1200	t	(0.602) $0.658^{+0.011\ +0.055}_{-0.008\ -0.043}$	(0.344) $0.529^{+0.070\ +0.041}_{-0.066\ -0.030}$
	$\bar{t}$	(0.244) $0.268^{+0.004\ +0.028}_{-0.003\ -0.025}$	(0.134) $0.209^{+0.025\ +0.021}_{-0.027\ -0.018}$
1400	t	(0.314) $0.342^{+0.006\ +0.034}_{-0.006\ -0.027}$	(0.170) $0.268^{+0.039\ +0.024}_{-0.034\ -0.018}$
	$\bar{t}$	(0.120) $0.132^{+0.003\ +0.017}_{-0.002\ -0.015}$	(0.063) $0.100^{+0.014\ +0.012}_{-0.013\ -0.010}$
1600	t	(0.168) $0.183^{+0.004\ +0.022}_{-0.003\ -0.017}$	(0.086) $0.141^{+0.021\ +0.015}_{-0.020\ -0.011}$
	$\bar{t}$	(0.061) $0.068^{+0.001\ +0.010}_{-0.002\ -0.009}$	(0.030) $0.050^{+0.008\ +0.007}_{-0.007\ -0.006}$
1800	t	(0.092) $0.100^{+0.003\ +0.014}_{-0.002\ -0.011}$	(0.045) $0.075^{+0.013\ +0.009}_{-0.011\ -0.006}$
	$\bar{t}$	(0.032) $0.035^{+0.001\ +0.006}_{-0.001\ -0.005}$	(0.015) $0.025^{+0.004\ +0.004}_{-0.004\ -0.003}$
2000	t	(0.051) $0.056^{+0.002\ +0.009}_{-0.002\ -0.007}$	(0.024) $0.041^{+0.007\ +0.005}_{-0.006\ -0.004}$
	$\bar{t}$	(0.017) $0.019^{+0.001\ +0.004}_{-0.001\ -0.003}$	(0.008) $0.013^{+0.002\ +0.002}_{-0.002\ -0.002}$

Table 5. Same as table 4 but for the MSTW2008 PDF set.

JHEP10(2009)042

top mass (GeV)		$2 \to 2$ (pb)	$2 \to 3$ (pb)
164	t	(146.1) $163.2^{+2.8\ +3.2}_{-2.7\ -3.7}$	(152.3) $156.5^{+5.2\ +3.0}_{-5.9\ -3.4}$
	$\bar{t}$	(85.1) $97.3^{+1.7\ +1.9}_{-1.5\ -2.2}$	(86.7) $92.8^{+2.6\ +1.8}_{-3.6\ -2.0}$
168	t	(141.9) $158.2^{+2.7\ +3.1}_{-2.6\ -3.6}$	(146.7) $151.9^{+5.0\ +2.9}_{-5.7\ -3.3}$
	$\bar{t}$	(82.4) $94.1^{+1.6\ +1.9}_{-1.5\ -2.2}$	(83.4) $89.8^{+2.8\ +1.8}_{-3.6\ -2.0}$
172	t	(137.6) $152.9^{+3.0\ +3.0}_{-2.3\ -3.4}$	(141.8) $147.0^{+5.0\ +2.7}_{-5.7\ -3.1}$
	$\bar{t}$	(79.8) $91.1^{+1.5\ +1.8}_{-1.5\ -2.1}$	(80.5) $86.8^{+2.4\ +1.8}_{-3.7\ -2.0}$
176	t	(133.6) $148.5^{+2.6\ +2.9}_{-2.3\ -3.3}$	(136.8) $142.6^{+4.9\ +2.7}_{-5.6\ -3.0}$
	$\bar{t}$	(77.5) $88.1^{+1.5\ +1.7}_{-1.3\ -2.0}$	(77.8) $83.6^{+2.7\ +1.6}_{-3.0\ -1.8}$
180	t	(129.6) $144.0^{+2.5\ +2.8}_{-2.2\ -3.2}$	(131.6) $138.1^{+4.9\ +2.6}_{-5.3\ -2.9}$
	$\bar{t}$	(75.0) $85.3^{+1.5\ +1.7}_{-1.2\ -2.0}$	(74.6) $81.1^{+2.1\ +1.6}_{-3.6\ -1.8}$
200	t	(112.2) $124.2^{+2.2\ +2.3}_{-1.7\ -2.6}$	(111.1) $117.0^{+4.4\ +2.1}_{-3.8\ -2.4}$
	$\bar{t}$	(64.5) $72.9^{+1.3\ +1.5}_{-1.0\ -1.7}$	(62.4) $68.9^{+2.1\ +1.4}_{-2.8\ -1.6}$
400	t	(34.5) $38.3^{+0.5\ +0.8}_{-0.3\ -0.8}$	(28.9) $35.2^{+1.9\ +0.8}_{-2.0\ -0.8}$
	$\bar{t}$	(18.4) $20.9^{+0.3\ +0.6}_{-0.1\ -0.7}$	(15.1) $19.1^{+0.7\ +0.6}_{-1.3\ -0.6}$
600	t	(14.01) $15.92^{+0.17\ +0.53}_{-0.09\ -0.51}$	(10.71) $14.25^{+0.94\ +0.48}_{-1.18\ -0.46}$
	$\bar{t}$	(7.06) $8.20^{+0.10\ +0.41}_{-0.04\ -0.42}$	(5.25) $7.18^{+0.44\ +0.37}_{-0.56\ -0.38}$
800	t	(6.60) $7.66^{+0.08\ +0.39}_{-0.05\ -0.35}$	(4.71) $6.64^{+0.60\ +0.34}_{-0.55\ -0.30}$
	$\bar{t}$	(3.15) $3.77^{+0.04\ +0.27}_{-0.02\ -0.26}$	(2.19) $3.20^{+0.25\ +0.24}_{-0.26\ -0.23}$
1000	t	(3.40) $4.05^{+0.04\ +0.28}_{-0.04\ -0.24}$	(2.30) $3.43^{+0.33\ +0.24}_{-0.31\ -0.20}$
	$\bar{t}$	(1.546) $1.907^{+0.019\ +0.179}_{-0.014\ -0.169}$	(1.020) $1.585^{+0.129\ +0.152}_{-0.143\ -0.142}$
1200	t	(1.86) $2.27^{+0.03\ +0.21}_{-0.02\ -0.17}$	(1.21) $1.90^{+0.19\ +0.17}_{-0.19\ -0.14}$
	$\bar{t}$	(0.810) $1.033^{+0.009\ +0.123}_{-0.009\ -0.112}$	(0.513) $0.842^{+0.070\ +0.100}_{-0.086\ -0.091}$
1400	t	(1.064) $1.333^{+0.016\ +0.149}_{-0.016\ -0.123}$	(0.663) $1.090^{+0.124\ +0.118}_{-0.117\ -0.096}$
	$\bar{t}$	(0.444) $0.585^{+0.006\ +0.085}_{-0.006\ -0.075}$	(0.270) $0.470^{+0.043\ +0.067}_{-0.053\ -0.060}$
1600	t	(0.626) $0.807^{+0.012\ +0.109}_{-0.010\ -0.089}$	(0.378) $0.651^{+0.074\ +0.083}_{-0.077\ -0.067}$
	$\bar{t}$	(0.252) $0.343^{+0.006\ +0.059}_{-0.003\ -0.051}$	(0.149) $0.268^{+0.034\ +0.044}_{-0.031\ -0.039}$
1800	t	(0.378) $0.503^{+0.008\ +0.080}_{-0.008\ -0.064}$	(0.221) $0.396^{+0.051\ +0.059}_{-0.046\ -0.047}$
	$\bar{t}$	(0.146) $0.208^{+0.004\ +0.041}_{-0.003\ -0.035}$	(0.084) $0.159^{+0.020\ +0.030}_{-0.019\ -0.026}$
2000	t	(0.233) $0.319^{+0.007\ +0.059}_{-0.005\ -0.047}$	(0.133) $0.251^{+0.030\ +0.042}_{-0.033\ -0.033}$
	$\bar{t}$	(0.087) $0.128^{+0.002\ +0.029}_{-0.002\ -0.024}$	(0.049) $0.096^{+0.014\ +0.021}_{-0.012\ -0.018}$

Table 6. NLO cross sections (pb) at the LHC 14 TeV for top and anti-top quarks production, as a function of the top mass obtained with the CTEQ6.6 PDF set and $V_{t^{(\prime)}b} = 1$. In the second (third) column the $2 \to 2$ ($2 \to 3$) results are shown, where the first uncertainty comes from renormalisation and factorisation scales variation and the second from PDF errors. Numbers in parenthesis refer to the corresponding LO results. These results are plotted in figure 4 where the scale and PDF uncertainties are combined linearly.

JHEP10(2009)042

top mass (GeV)		$2 \to 2$ (pb)	$2 \to 3$ (pb)
164	t	(148.1) $164.1^{+3.1\ +2.4}_{-2.8\ -2.4}$	(155.1) $157.8^{+4.4\ +2.4}_{-6.9\ -2.3}$
	$\bar{t}$	(88.8) $100.6^{+1.7\ +1.3}_{-1.8\ -2.0}$	(91.4) $95.5^{+2.2\ +1.4}_{-4.1\ -1.9}$
168	t	(143.7) $159.3^{+2.6\ +2.3}_{-2.9\ -2.3}$	(149.1) $152.1^{+4.7\ +2.4}_{-5.9\ -2.2}$
	$\bar{t}$	(86.1) $97.3^{+1.7\ +1.3}_{-1.6\ -1.9}$	(87.6) $91.7^{+2.6\ +1.3}_{-3.5\ -1.8}$
172	t	(139.4) $154.3^{+2.9\ +2.2}_{-2.5\ -2.2}$	(143.9) $146.8^{+4.3\ +2.2}_{-5.0\ -2.1}$
	$\bar{t}$	(83.4) $94.2^{+1.6\ +1.2}_{-1.5\ -1.9}$	(84.6) $88.7^{+2.6\ +1.3}_{-3.0\ -1.8}$
176	t	(135.2) $149.6^{+2.6\ +2.1}_{-2.4\ -2.1}$	(138.9) $142.7^{+4.6\ +2.2}_{-6.1\ -2.0}$
	$\bar{t}$	(80.8) $91.1^{+1.6\ +1.2}_{-1.4\ -1.8}$	(81.4) $85.8^{+2.1\ +1.2}_{-3.5\ -1.7}$
180	t	(131.3) $145.2^{+2.5\ +2.0}_{-2.3\ -2.0}$	(134.1) $138.6^{+5.1\ +2.1}_{-5.6\ -1.9}$
	$\bar{t}$	(78.4) $88.2^{+1.6\ +1.2}_{-1.3\ -1.8}$	(78.5) $83.1^{+2.1\ +1.2}_{-3.4\ -1.6}$
200	t	(113.6) $125.5^{+2.0\ +1.7}_{-1.9\ -1.7}$	(112.8) $119.3^{+3.7\ +1.7}_{-5.4\ -1.6}$
	$\bar{t}$	(67.4) $75.5^{+1.2\ +1.0}_{-1.1\ -1.5}$	(65.5) $70.9^{+2.1\ +1.0}_{-3.1\ -1.4}$
400	t	(35.1) $38.9^{+0.5\ +0.6}_{-0.2\ -0.5}$	(29.5) $35.6^{+2.1\ +0.5}_{-2.1\ -0.4}$
	$\bar{t}$	(19.5) $21.7^{+0.3\ +0.5}_{-0.1\ -0.6}$	(15.9) $19.6^{+0.9\ +0.5}_{-1.3\ -0.5}$
600	t	(14.51) $16.22^{+0.19\ +0.38}_{-0.10\ -0.30}$	(11.01) $14.42^{+0.98\ +0.34}_{-1.15\ -0.25}$
	$\bar{t}$	(7.61) $8.49^{+0.11\ +0.28}_{-0.05\ -0.31}$	(5.58) $7.36^{+0.48\ +0.25}_{-0.58\ -0.26}$
800	t	(6.97) $7.81^{+0.08\ +0.26}_{-0.05\ -0.21}$	(4.91) $6.78^{+0.54\ +0.22}_{-0.64\ -0.17}$
	$\bar{t}$	(3.46) $3.88^{+0.04\ +0.17}_{-0.03\ -0.18}$	(2.34) $3.29^{+0.26\ +0.15}_{-0.31\ -0.15}$
1000	t	(3.66) $4.11^{+0.05\ +0.18}_{-0.03\ -0.15}$	(2.42) $3.50^{+0.31\ +0.15}_{-0.36\ -0.11}$
	$\bar{t}$	(1.732) $1.945^{+0.018\ +0.112}_{-0.015\ -0.111}$	(1.101) $1.604^{+0.158\ +0.092}_{-0.162\ -0.087}$
1200	t	(2.05) $2.30^{+0.03\ +0.13}_{-0.03\ -0.10}$	(1.28) $1.89^{+0.20\ +0.10}_{-0.20\ -0.07}$
	$\bar{t}$	(0.925) $1.040^{+0.011\ +0.074}_{-0.009\ -0.070}$	(0.556) $0.831^{+0.087\ +0.058}_{-0.088\ -0.053}$
1400	t	(1.192) $1.339^{+0.020\ +0.089}_{-0.014\ -0.071}$	(0.709) $1.088^{+0.123\ +0.068}_{-0.126\ -0.050}$
	$\bar{t}$	(0.516) $0.583^{+0.007\ +0.049}_{-0.007\ -0.046}$	(0.296) $0.458^{+0.051\ +0.037}_{-0.054\ -0.033}$
1600	t	(0.718) $0.806^{+0.014\ +0.063}_{-0.010\ -0.050}$	(0.409) $0.642^{+0.079\ +0.047}_{-0.078\ -0.033}$
	$\bar{t}$	(0.299) $0.337^{+0.005\ +0.033}_{-0.004\ -0.030}$	(0.164) $0.259^{+0.032\ +0.024}_{-0.030\ -0.021}$
1800	t	(0.443) $0.497^{+0.010\ +0.045}_{-0.008\ -0.035}$	(0.242) $0.389^{+0.050\ +0.032}_{-0.049\ -0.023}$
	$\bar{t}$	(0.177) $0.200^{+0.004\ +0.023}_{-0.003\ -0.020}$	(0.093) $0.151^{+0.019\ +0.016}_{-0.018\ -0.014}$
2000	t	(0.279) $0.312^{+0.007\ +0.032}_{-0.006\ -0.025}$	(0.147) $0.240^{+0.033\ +0.022}_{-0.031\ -0.016}$
	$\bar{t}$	(0.107) $0.121^{+0.003\ +0.016}_{-0.002\ -0.014}$	(0.054) $0.089^{+0.013\ +0.011}_{-0.012\ -0.009}$

Table 7. Same as table 6 but for the MSTW2008 PDF set.

JHEP10(2009)042

B Cross sections and uncertainties for tb' and $t'b'$ production

$m_{b'}$ (GeV)		cross section (fb)
200	$b'\bar{t}$	(9394) $9556^{+105\ +202}_{-317\ -203}$
	$\bar{b}'t$	(5211) $5334^{+41\ +173}_{-131\ -193}$
400	$b'\bar{t}$	(3256) $3607^{+82\ +132}_{-172\ -120}$
	$\bar{b}'t$	(1696) $1907^{+18\ +98}_{-89\ -102}$
600	$b'\bar{t}$	(1457) $1738^{+54\ +92}_{-105\ -79}$
	$\bar{b}'t$	(713) $863^{+17\ +64}_{-44\ -63}$
800	$b'\bar{t}$	(729) $920^{+41\ +64}_{-61\ -54}$
	$\bar{b}'t$	(338) $435^{+13\ +41}_{-27\ -39}$
1000	$b'\bar{t}$	(390) $518^{+29\ +46}_{-37\ -38}$
	$\bar{b}'t$	(172) $235^{+9\ +28}_{-18\ -26}$
1200	$b'\bar{t}$	(219) $307^{+16\ +32}_{-27\ -26}$
	$\bar{b}'t$	(92.0) $132.1^{+7.2\ +19.9}_{-10.7\ -18.3}$
1400	$b'\bar{t}$	(126.5) $184.6^{+13.6\ +23.2}_{-16.1\ -18.4}$
	$\bar{b}'t$	(51.1) $77.7^{+4.4\ +13.0}_{-7.0\ -11.7}$
1600	$b'\bar{t}$	(75.1) $114.4^{+9.5\ +16.5}_{-10.5\ -13.0}$
	$\bar{b}'t$	(29.2) $46.7^{+2.7\ +8.7}_{-4.6\ -7.5}$
1800	$b'\bar{t}$	(45.5) $72.5^{+6.7\ +11.9}_{-7.2\ -9.3}$
	$\bar{b}'t$	(17.0) $28.5^{+2.1\ +6.0}_{-2.8\ -5.1}$
2000	$b'\bar{t}$	(28.0) $46.8^{+3.9\ +8.5}_{-5.2\ -6.5}$
	$\bar{b}'t$	(10.10) $17.90^{+1.39\ +4.18}_{-1.95\ -3.52}$

Table 8. NLO cross sections (fb) at the LHC 14 TeV for $b'\bar{t}$ and $\bar{b}'t$ as a function of $m_{b'}$ obtained with the CTEQ6.6 PDF set and $V_{tb'} = 1$. The first uncertainty comes from renormalisation and factorisation scales variation and the second from PDF errors. Numbers in parenthesis refer to the corresponding LO results. These results are plotted in figure 5 where the scale and PDF uncertainties are combined linearly.

JHEP10(2009)042

$m_{b'}$ (GeV)		cross section (fb)
200	$b'\bar{t}$	(9719) $9797^{+121\ +160}_{-315\ -121}$
	$\bar{b}'t$	(5551) $5575^{+27\ +133}_{-121\ -142}$
400	$b'\bar{t}$	(3401) $3696^{+73\ +92}_{-184\ -64}$
	$\bar{b}'t$	(1820) $1959^{+49\ +66}_{-73\ -67}$
600	$b'\bar{t}$	(1537) $1771^{+66\ +60}_{-104\ -42}$
	$\bar{b}'t$	(772) $884^{+31\ +39}_{-41\ -38}$
800	$b'\bar{t}$	(777) $937^{+41\ +40}_{-65\ -28}$
	$\bar{b}'t$	(369) $441^{+15\ +24}_{-27\ -21}$
1000	$b'\bar{t}$	(421) $526^{+29\ +27}_{-43\ -20}$
	$\bar{b}'t$	(189) $235^{+11\ +16}_{-18\ -14}$
1200	$b'\bar{t}$	(238) $307^{+19\ +19}_{-28\ -13}$
	$\bar{b}'t$	(102.0) $131.4^{+7.7\ +10.4}_{-11.3\ -9.1}$
1400	$b'\bar{t}$	(139.1) $183.6^{+13.2\ +13.1}_{-16.8\ -9.1}$
	$\bar{b}'t$	(57.0) $75.0^{+5.7\ +6.9}_{-6.7\ -6.0}$
1600	$b'\bar{t}$	(83.4) $112.7^{+10.2\ +9.1}_{-11.0\ -6.3}$
	$\bar{b}'t$	(32.7) $44.1^{+3.1\ +4.5}_{-4.1\ -3.8}$
1800	$b'\bar{t}$	(51.0) $70.9^{+6.1\ +6.3}_{-7.8\ -4.4}$
	$\bar{b}'t$	(19.2) $26.4^{+2.7\ +3.0}_{-2.5\ -2.4}$
2000	$b'\bar{t}$	(31.7) $44.6^{+4.7\ +4.4}_{-4.9\ -3.0}$
	$\bar{b}'t$	(11.46) $16.23^{+1.56\ +2.08}_{-1.80\ -1.71}$

Table 9. Same as table 8 but for the MSTW2008 PDF set.

JHEP10(2009)042

$m_{t'}$ (GeV)		$m_{b'} = m_{t'}$	$m_{t'} - m_{b'}$=200 GeV	$m_{t'} - m_{b'}$=500 GeV
172	$t'\bar{b}'$	(11423) $11503^{+116\ +235}_{-359\ -240}$	–	–
	$\bar{t}'b'$	(6381) $6479^{+31\ +180}_{-150\ -205}$	–	–
200	$t'\bar{b}'$	(7777) $8011^{+110\ +183}_{-313\ -183}$	–	–
	$\bar{t}'b'$	(4239) $4391^{+24\ +155}_{-124\ -171}$	–	–
400	$t'\bar{b}'$	(992) $1147^{+27\ +64}_{-60\ -55}$	(2763) $3072^{+74\ +117}_{-134\ -106}$	–
	$\bar{t}'b'$	(470) $553^{+10\ +42}_{-29\ -41}$	(1370) $1547^{+15\ +86}_{-70\ -87}$	–
600	$t'\bar{b}'$	(219) $279^{+10\ +25}_{-19\ -21}$	(465) $565^{+21\ +41}_{-31\ -34}$	(2538) $3022^{+114\ +138}_{-179\ -122}$
	$\bar{t}'b'$	(93.7) $121.7^{+4.7\ +16.2}_{-6.3\ -15.6}$	(207.3) $258.2^{+6.3\ +25.7}_{-14.7\ -24.3}$	(1207.3) $1474.6^{+34.2\ +95.4}_{-82.6\ -94.9}$
800	$t'\bar{b}'$	(61.6) $85.5^{+4.1\ +10.9}_{-7.1\ -8.6}$	(116.1) $154.3^{+5.9\ +16.7}_{-11.2\ -13.5}$	(377.5) $479.3^{+19.6\ +39.0}_{-30.1\ -32.2}$
	$\bar{t}'b'$	(24.2) $34.6^{+1.3\ +5.8}_{-2.5\ -5.1}$	(47.3) $64.6^{+2.5\ +9.5}_{-4.5\ -8.5}$	(163.2) $213.2^{+7.1\ +23.2}_{-15.0\ -22.2}$
1000	$t'\bar{b}'$	(19.8) $29.7^{+1.8\ +4.9}_{-2.6\ -3.8}$	(34.9) $50.2^{+2.8\ +7.4}_{-4.3\ -5.8}$	(92.7) $126.7^{+7.1\ +15.0}_{-9.4\ -12.0}$
	$\bar{t}'b'$	(7.19) $11.26^{+0.66\ +2.44}_{-0.88\ -2.09}$	(13.15) $19.80^{+0.91\ +3.80}_{-1.59\ -3.29}$	(36.86) $52.55^{+1.43\ +8.20}_{-4.17\ -7.28}$
1200	$t'\bar{b}'$	(6.90) $11.21^{+0.80\ +2.32}_{-1.12\ -1.76}$	(11.69) $18.24^{+1.28\ +3.37}_{-1.69\ -2.57}$	(27.87) $41.23^{+2.51\ +6.49}_{-3.71\ -5.05}$
	$\bar{t}'b'$	(2.34) $4.08^{+0.24\ +1.08}_{-0.38\ -0.90}$	(4.09) $6.78^{+0.33\ +1.63}_{-0.62\ -1.37}$	(10.28) $16.05^{+0.60\ +3.26}_{-1.54\ -2.80}$
1400	$t'\bar{b}'$	(2.54) $4.47^{+0.38\ +1.12}_{-0.48\ -0.84}$	(4.19) $7.09^{+0.54\ +1.61}_{-0.72\ -1.21}$	(9.37) $14.91^{+1.17\ +2.93}_{-1.39\ -2.24}$
	$\bar{t}'b'$	(0.80) $1.54^{+0.10\ +0.49}_{-0.16\ -0.40}$	(1.37) $2.51^{+0.15\ +0.73}_{-0.26\ -0.60}$	(3.22) $5.44^{+0.39\ +1.42}_{-0.48\ -1.20}$
1600	$t'\bar{b}'$	(0.97) $1.86^{+0.16\ +0.54}_{-0.22\ -0.40}$	(1.57) $2.88^{+0.25\ +0.77}_{-0.31\ -0.57}$	(3.37) $5.83^{+0.47\ +1.38}_{-0.61\ -1.04}$
	$\bar{t}'b'$	(0.29) $0.61^{+0.05\ +0.23}_{-0.07\ -0.18}$	(0.48) $0.96^{+0.07\ +0.34}_{-0.10\ -0.27}$	(1.08) $2.03^{+0.14\ +0.61}_{-0.22\ -0.50}$
1800	$t'\bar{b}'$	(0.38) $0.79^{+0.08\ +0.27}_{-0.10\ -0.19}$	(0.61) $1.21^{+0.13\ +0.38}_{-0.14\ -0.28}$	(1.26) $2.37^{+0.21\ +0.66}_{-0.25\ -0.49}$
	$\bar{t}'b'$	(0.10) $0.24^{+0.03\ +0.11}_{-0.03\ -0.08}$	(0.17) $0.38^{+0.04\ +0.15}_{-0.04\ -0.12}$	(0.38) $0.78^{+0.07\ +0.28}_{-0.09\ -0.23}$
2000	$t'\bar{b}'$	(0.15) $0.34^{+0.04\ +0.13}_{-0.04\ -0.09}$	(0.24) $0.52^{+0.06\ +0.19}_{-0.07\ -0.14}$	(0.49) $0.99^{+0.10\ +0.33}_{-0.12\ -0.24}$
	$\bar{t}'b'$	(0.04) $0.10^{+0.01\ +0.05}_{-0.01\ -0.04}$	(0.06) $0.16^{+0.02\ +0.08}_{-0.02\ -0.06}$	(0.14) $0.31^{+0.03\ +0.13}_{-0.03\ -0.10}$

Table 10. NLO cross sections (fb) at the LHC 14 TeV for $t'\bar{b}'$ and $\bar{t}'b'$ as a function of $m_{t'}$ obtained with the CTEQ6.6 PDF set and $V_{t'b'} = 1$. The first uncertainty comes from renormalisation and factorisation scales variation and the second from PDF errors. Numbers in parenthesis refer to the corresponding LO results. These results are plotted in figure 6 where the scale and PDF uncertainties are combined linearly.

JHEP10(2009)042

$m_{t'}$ (GeV)		$m_{b'} = m_{t'}$	$m_{t'} - m_{b'}$=200 GeV	$m_{t'} - m_{b'}$=500 GeV
172	$t'\bar{b}'$	(11808) $11795^{+115\ +185}_{-369\ -140}$	–	–
	$\bar{t}'b'$	(6793) $6741^{+48\ +161}_{-173\ -172}$	–	–
200	$t'\bar{b}'$	(8058) $8220^{+76\ +143}_{-309\ -107}$	–	–
	$\bar{t}'b'$	(4522) $4584^{+29\ +115}_{-154\ -122}$	–	–
400	$t'\bar{b}'$	(1047) $1173^{+24\ +41}_{-69\ -28}$	(2887) $3149^{+58\ +81}_{-156\ -57}$	–
	$\bar{t}'b'$	(510) $570^{+5\ +28}_{-29\ -26}$	(1476) $1597^{+19\ +56}_{-65\ -57}$	–
600	$t'\bar{b}'$	(237) $280^{+11\ +15}_{-18\ -10}$	(497) $577^{+19\ +26}_{-39\ -17}$	(2660) $3105^{+111\ +92}_{-200\ -65}$
	$\bar{t}'b'$	(103.4) $121.7^{+4.6\ +8.6}_{-7.7\ -7.6}$	(227.2) $262.1^{+8.6\ +15.3}_{-16.0\ -14.1}$	(1306.1) $1514.7^{+49.9\ +61.7}_{-85.2\ -61.5}$
800	$t'\bar{b}'$	(67.9) $84.3^{+4.2\ +6.1}_{-7.2\ -4.1}$	(126.7) $154.6^{+6.2\ +9.7}_{-12.6\ -6.6}$	(405.1) $484.2^{+20.2\ +23.8}_{-34.0\ -16.3}$
	$\bar{t}'b'$	(27.1) $33.4^{+1.7\ +3.1}_{-2.6\ -2.7}$	(52.6) $63.7^{+2.4\ +5.2}_{-4.7\ -4.5}$	(179.5) $213.9^{+7.1\ +13.5}_{-13.5\ -12.3}$
1000	$t'\bar{b}'$	(22.2) $28.7^{+1.8\ +2.6}_{-2.7\ -1.8}$	(38.9) $49.0^{+3.2\ +4.0}_{-4.2\ -2.7}$	(101.7) $126.2^{+6.5\ +8.5}_{-10.4\ -5.8}$
	$\bar{t}'b'$	(8.15) $10.55^{+0.60\ +1.26}_{-1.03\ -1.04}$	(14.82) $18.71^{+0.96\ +1.96}_{-1.48\ -1.63}$	(41.13) $51.02^{+2.51\ +4.58}_{-3.98\ -3.95}$
1200	$t'\bar{b}'$	(7.90) $10.56^{+0.80\ +1.13}_{-1.11\ -0.76}$	(13.26) $17.38^{+1.25\ +1.71}_{-1.71\ -1.16}$	(31.18) $39.97^{+2.67\ +3.42}_{-3.61\ -2.33}$
	$\bar{t}'b'$	(2.67) $3.57^{+0.23\ +0.51}_{-0.37\ -0.41}$	(4.66) $6.12^{+0.39\ +0.79}_{-0.60\ -0.65}$	(11.61) $15.06^{+0.60\ +1.67}_{-1.52\ -1.39}$
1400	$t'\bar{b}'$	(2.95) $4.04^{+0.37\ +0.51}_{-0.45\ -0.35}$	(4.83) $6.53^{+0.57\ +0.76}_{-0.70\ -0.52}$	(10.66) $14.12^{+1.13\ +1.45}_{-1.37\ -0.99}$
	$\bar{t}'b'$	(0.93) $1.26^{+0.12\ +0.21}_{-0.13\ -0.17}$	(1.57) $2.13^{+0.19\ +0.33}_{-0.22\ -0.26}$	(3.67) $4.88^{+0.28\ +0.66}_{-0.50\ -0.54}$
1600	$t'\bar{b}'$	(1.14) $1.61^{+0.17\ +0.23}_{-0.19\ -0.16}$	(1.84) $2.55^{+0.26\ +0.34}_{-0.29\ -0.23}$	(3.89) $5.32^{+0.50\ +0.64}_{-0.60\ -0.44}$
	$\bar{t}'b'$	(0.33) $0.47^{+0.04\ +0.09}_{-0.06\ -0.07}$	(0.55) $0.77^{+0.08\ +0.14}_{-0.09\ -0.11}$	(1.24) $1.70^{+0.15\ +0.27}_{-0.20\ -0.22}$
1800	$t'\bar{b}'$	(0.45) $0.65^{+0.07\ +0.10}_{-0.08\ -0.07}$	(0.72) $1.02^{+0.11\ +0.15}_{-0.12\ -0.11}$	(1.48) $2.08^{+0.19\ +0.29}_{-0.26\ -0.20}$
	$\bar{t}'b'$	(0.12) $0.17^{+0.02\ +0.04}_{-0.02\ -0.03}$	(0.20) $0.28^{+0.03\ +0.06}_{-0.04\ -0.05}$	(0.44) $0.61^{+0.07\ +0.12}_{-0.07\ -0.09}$
2000	$t'\bar{b}'$	(0.18) $0.27^{+0.04\ +0.05}_{-0.04\ -0.03}$	(0.28) $0.42^{+0.05\ +0.07}_{-0.05\ -0.05}$	(0.58) $0.83^{+0.09\ +0.13}_{-0.11\ -0.09}$
	$\bar{t}'b'$	(0.04) $0.07^{+0.01\ +0.02}_{-0.01\ -0.01}$	(0.07) $0.11^{+0.01\ +0.03}_{-0.01\ -0.02}$	(0.16) $0.23^{+0.02\ +0.05}_{-0.03\ -0.04}$

Table 11. Same as table 10 but for the MSTW2008 PDF set.

JHEP10(2009)042

$m_{b'}$ (GeV)		$m_{b'} - m_{t'}$=200 GeV	$m_{b'} - m_{t'}$=500 GeV
400	$b'\bar{t}'$	(1394) $1568^{+10\ +87}_{-74\ -89}$	–
	$\bar{b}'t'$	(2712) $3012^{+65\ +116}_{-147\ -104}$	–
600	$b'\bar{t}'$	(209) $260^{+6\ +26}_{-16\ -24}$	–
	$\bar{b}'t'$	(462) $565^{+19\ +41}_{-36\ -34}$	–
800	$b'\bar{t}'$	(47.5) $65.2^{+2.3\ +9.4}_{-4.9\ -8.5}$	(165.5) $215.0^{+5.2\ +23.1}_{-14.0\ -21.3}$
	$\bar{b}'t'$	(115.6) $153.7^{+7.5\ +16.6}_{-10.8\ -13.4}$	(371.8) $472.6^{+19.6\ +38.7}_{-32.7\ -31.9}$
1000	$b'\bar{t}'$	(13.18) $19.79^{+1.00\ +3.78}_{-1.60\ -3.25}$	(37.17) $52.68^{+1.66\ +8.20}_{-3.98\ -7.26}$
	$\bar{b}'t'$	(34.8) $50.3^{+2.5\ +7.4}_{-4.3\ -5.8}$	(91.9) $125.6^{+6.6\ +15.0}_{-9.3\ -12.0}$
1200	$b'\bar{t}'$	(4.10) $6.76^{+0.39\ +1.63}_{-0.60\ -1.37}$	(10.33) $16.07^{+0.79\ +3.18}_{-1.34\ -2.70}$
	$\bar{b}'t'$	(11.67) $18.15^{+1.19\ +3.40}_{-1.64\ -2.60}$	(27.69) $40.97^{+2.60\ +6.37}_{-3.49\ -4.95}$
1400	$b'\bar{t}'$	(1.37) $2.48^{+0.18\ +0.94}_{-0.25\ -0.76}$	(3.23) $5.49^{+0.39\ +1.38}_{-0.50\ -1.15}$
	$\bar{b}'t'$	(4.18) $7.10^{+0.52\ +1.61}_{-0.74\ -1.21}$	(9.32) $14.85^{+1.14\ +2.93}_{-1.36\ -2.24}$
1600	$b'\bar{t}'$	(0.48) $0.96^{+0.08\ +0.34}_{-0.10\ -0.27}$	(1.08) $2.03^{+0.15\ +0.62}_{-0.20\ -0.51}$
	$\bar{b}'t'$	(1.57) $2.88^{+0.25\ +0.78}_{-0.32\ -0.57}$	(3.35) $5.80^{+0.49\ +1.38}_{-0.59\ -1.03}$
1800	$b'\bar{t}'$	(0.17) $0.39^{+0.03\ +0.16}_{-0.05\ -0.12}$	(0.38) $0.78^{+0.07\ +0.28}_{-0.09\ -0.23}$
	$\bar{b}'t'$	(0.61) $1.21^{+0.12\ +0.38}_{-0.14\ -0.28}$	(1.26) $2.37^{+0.22\ +0.67}_{-0.27\ -0.49}$
2000	$b'\bar{t}'$	(0.06) $0.16^{+0.02\ +0.07}_{-0.02\ -0.06}$	(0.14) $0.31^{+0.03\ +0.15}_{-0.04\ -0.13}$
	$\bar{b}'t'$	(0.24) $0.52^{+0.06\ +0.19}_{-0.07\ -0.14}$	(0.49) $0.99^{+0.10\ +0.33}_{-0.12\ -0.24}$

Table 12. Cross sections (fb) at the LHC 14 TeV for $b'\bar{t}'$ and $\bar{b}'t'$ as a function of $m_{b'}$ obtained with the CTEQ6.6 PDF set and $V_{t'b'} = 1$. The first uncertainty comes from renormalisation and factorisation scales variation and the second from PDF errors. Numbers in parenthesis refer to the corresponding LO results. These results are plotted in figure 7 where the scale and PDF uncertainties are combined linearly.

JHEP10(2009)042

$m_{b'}$ (GeV)		$m_{b'} - m_{t'}$=200 GeV	$m_{b'} - m_{t'}$=500 GeV
400	$b'\bar{t}'$	(1498) $1616^{+28\ +57}_{-58\ -58}$	–
	$\bar{b}'t'$	(2837) $3096^{+66\ +80}_{-160\ -56}$	–
600	$b'\bar{t}'$	(229) $265^{+5\ +15}_{-16\ -14}$	–
	$\bar{b}'t'$	(493) $572^{+19\ +25}_{-37\ -17}$	–
800	$b'\bar{t}'$	(52.8) $64.0^{+2.1\ +5.1}_{-4.6\ -4.4}$	(181.7) $217.5^{+6.8\ +14.2}_{-15.8\ -13.0}$
	$\bar{b}'t'$	(126.2) $153.8^{+6.8\ +9.7}_{-12.5\ -6.6}$	(399.2) $480.0^{+19.9\ +23.7}_{-35.4\ -15.9}$
1000	$b'\bar{t}'$	(14.84) $18.68^{+1.11\ +1.97}_{-1.56\ -1.66}$	(41.44) $51.09^{+2.15\ +4.51}_{-3.91\ -3.89}$
	$\bar{b}'t'$	(38.8) $49.0^{+3.2\ +4.0}_{-4.1\ -2.7}$	(100.8) $125.2^{+6.7\ +8.4}_{-10.2\ -5.7}$
1200	$b'\bar{t}'$	(4.67) $6.07^{+0.44\ +0.79}_{-0.55\ -0.65}$	(11.67) $15.09^{+0.78\ +1.67}_{-1.50\ -1.39}$
	$\bar{b}'t'$	(13.24) $17.28^{+1.43\ +1.71}_{-1.66\ -1.17}$	(31.00) $39.80^{+2.57\ +3.39}_{-3.69\ -2.29}$
1400	$b'\bar{t}'$	(1.57) $2.13^{+0.17\ +0.36}_{-0.22\ -0.29}$	(3.68) $4.89^{+0.33\ +0.66}_{-0.51\ -0.54}$
	$\bar{b}'t'$	(4.83) $6.53^{+0.60\ +0.76}_{-0.70\ -0.52}$	(10.62) $14.05^{+1.19\ +1.45}_{-1.41\ -0.99}$
1600	$b'\bar{t}'$	(0.55) $0.76^{+0.08\ +0.14}_{-0.08\ -0.11}$	(1.24) $1.70^{+0.16\ +0.28}_{-0.18\ -0.22}$
	$\bar{b}'t'$	(1.83) $2.55^{+0.26\ +0.34}_{-0.29\ -0.23}$	(3.88) $5.30^{+0.48\ +0.64}_{-0.60\ -0.44}$
1800	$b'\bar{t}'$	(0.20) $0.28^{+0.04\ +0.06}_{-0.03\ -0.05}$	(0.44) $0.62^{+0.05\ +0.12}_{-0.08\ -0.09}$
	$\bar{b}'t'$	(0.72) $1.02^{+0.11\ +0.15}_{-0.13\ -0.11}$	(1.48) $2.07^{+0.22\ +0.29}_{-0.25\ -0.20}$
2000	$b'\bar{t}'$	(0.07) $0.11^{+0.01\ +0.03}_{-0.01\ -0.02}$	(0.16) $0.23^{+0.03\ +0.05}_{-0.03\ -0.04}$
	$\bar{b}'t'$	(0.28) $0.41^{+0.05\ +0.07}_{-0.05\ -0.05}$	(0.58) $0.83^{+0.10\ +0.13}_{-0.10\ -0.09}$

Table 13. Same as table 12 but for the MSTW2008 PDF set.

References

[1] CDF collaboration, T. Aaltonen et al., *First observation of electroweak single top quark production*, *Phys. Rev. Lett.* **103** (2009) 092002 [arXiv:0903.0885] [SPIRES].

[2] D0 collaboration, V.M. Abazov et al., *Observation of single top-quark production*, *Phys. Rev. Lett.* **103** (2009) 092001 [arXiv:0903.0850] [SPIRES].

[3] J. Alwall et al., *Is* $V_{tb} \simeq 1$*?*, *Eur. Phys. J.* **C 49** (2007) 791 [hep-ph/0607115] [SPIRES].

[4] T.M.P. Tait and C.P. Yuan, *Single top quark production as a window to physics beyond the standard model*, *Phys. Rev.* **D 63** (2001) 014018 [hep-ph/0007298] [SPIRES].

[5] E.A. Mirabelli and M. Schmaltz, *Yukawa hierarchies from split fermions in extra dimensions*, *Phys. Rev.* **D 61** (2000) 113011 [hep-ph/9912265] [SPIRES].

[6] N. Arkani-Hamed et al., *The minimal Moose for a little Higgs*, *JHEP* **08** (2002) 021 [hep-ph/0206020] [SPIRES].

[7] T. Han, H.E. Logan, B. McElrath and L.-T. Wang, *Phenomenology of the little Higgs model*, *Phys. Rev.* **D 67** (2003) 095004 [hep-ph/0301040] [SPIRES].

JHEP10(2009)042

[8] K. Agashe, R. Contino, L. Da Rold and A. Pomarol, *A custodial symmetry for $Zb\bar{b}$*, *Phys. Lett.* **B 641** (2006) 62 [hep-ph/0605341] [SPIRES].

[9] J.A. Aguilar-Saavedra, *Pair production of heavy $Q = 2/3$ singlets at LHC*, *Phys. Lett.* **B 625** (2005) 234 [*Erratum ibid.* **B 633** (2006) 792] [hep-ph/0506187] [SPIRES].

[10] R. Contino and G. Servant, *Discovering the top partners at the LHC using same-sign dilepton final states*, *JHEP* **06** (2008) 026 [arXiv:0801.1679] [SPIRES].

[11] J.A. Aguilar-Saavedra, *Identifying top partners at LHC*, arXiv:0907.3155 [SPIRES].

[12] G.D. Kribs, T. Plehn, M. Spannowsky and T.M.P. Tait, *Four generations and Higgs physics*, *Phys. Rev.* **D 76** (2007) 075016 [arXiv:0706.3718] [SPIRES].

[13] A. Soni, A.K. Alok, A. Giri, R. Mohanta and S. Nandi, *The fourth family: a natural explanation for the observed pattern of anomalies in B^- CP asymmetries*, arXiv:0807.1971 [SPIRES].

[14] M.S. Chanowitz, *Bounding CKM mixing with a fourth family*, *Phys. Rev.* **D 79** (2009) 113008 [arXiv:0904.3570] [SPIRES].

[15] B. Holdom et al., *Four statements about the fourth generation*, arXiv:0904.4698 [SPIRES].

[16] A. Soni, *The '4$^{\text{th}}$ generation', B-CP anomalies & the LHC*, arXiv:0907.2057 [SPIRES].

[17] Particle Data Group collaboration, C. Amsler et al., *Review of particle physics*, *Phys. Lett.* **B 667** (2008) 1 [SPIRES].

[18] J.M. Campbell, R. Frederix, F. Maltoni and F. Tramontano, *Next-to-leading-order predictions for t-channel single-top production at hadron colliders*, *Phys. Rev. Lett.* **102** (2009) 182003 [arXiv:0903.0005] [SPIRES].

[19] G. Bordes and B. van Eijk, *Calculating QCD corrections to single top production in hadronic interactions*, *Nucl. Phys.* **B 435** (1995) 23 [SPIRES].

[20] T. Stelzer, Z. Sullivan and S. Willenbrock, *Single top quark production via W-gluon fusion at next-to-leading order*, *Phys. Rev.* **D 56** (1997) 5919 [hep-ph/9705398] [SPIRES].

[21] B.W. Harris, E. Laenen, L. Phaf, Z. Sullivan and S. Weinzierl, *The fully differential single top quark cross-section in next to leading order QCD*, *Phys. Rev.* **D 66** (2002) 054024 [hep-ph/0207055] [SPIRES].

[22] J.M. Campbell, R.K. Ellis and F. Tramontano, *Single top production and decay at next-to-leading order*, *Phys. Rev.* **D 70** (2004) 094012 [hep-ph/0408158] [SPIRES].

[23] Q.-H. Cao, R. Schwienhorst and C.P. Yuan, *Next-to-leading order corrections to single top quark production and decay at Tevatron. 1. s^- channel process*, *Phys. Rev.* **D 71** (2005) 054023 [hep-ph/0409040] [SPIRES].

[24] Q.-H. Cao, R. Schwienhorst, J.A. Benitez, R. Brock and C.P. Yuan, *Next-to-leading order corrections to single top quark production and decay at the Tevatron: 2. t^- channel process*, *Phys. Rev.* **D 72** (2005) 094027 [hep-ph/0504230] [SPIRES].

[25] S. Frixione, E. Laenen, P. Motylinski and B.R. Webber, *Single-top production in MC@NLO*, *JHEP* **03** (2006) 092 [hep-ph/0512250] [SPIRES].

[26] M. Beccaria, G. Macorini, F.M. Renard and C. Verzegnassi, *Single top production in the t-channel at LHC: a realistic test of electroweak models*, *Phys. Rev.* **D 74** (2006) 013008 [hep-ph/0605108] [SPIRES].

JHEP10(2009)042

[27] M. Beccaria et al., *A complete one-loop calculation of electroweak supersymmetric effects in t-channel single top production at LHC*, *Phys. Rev.* **D 77** (2008) 113018 [arXiv:0802.1994] [SPIRES].

[28] M. Cacciari, S. Frixione, M.L. Mangano, P. Nason and G. Ridolfi, *Updated predictions for the total production cross sections of top and of heavier quark pairs at the Tevatron and at the LHC*, *JHEP* **09** (2008) 127 [arXiv:0804.2800] [SPIRES].

[29] F. Maltoni, Z. Sullivan and S. Willenbrock, *Higgs-boson production via bottom-quark fusion*, *Phys. Rev.* **D 67** (2003) 093005 [hep-ph/0301033] [SPIRES].

[30] J.M. Campbell et al., *Higgs boson production in association with bottom quarks*, hep-ph/0405302 [SPIRES].

[31] N. Kidonakis, *Single top production at the Tevatron: threshold resummation and finite-order soft gluon corrections*, *Phys. Rev.* **D 74** (2006) 114012 [hep-ph/0609287] [SPIRES].

[32] N. Kidonakis, *Higher-order soft gluon corrections in single top quark production at the LHC*, *Phys. Rev.* **D 75** (2007) 071501 [hep-ph/0701080] [SPIRES].

[33] P.M. Nadolsky et al., *Implications of CTEQ global analysis for collider observables*, *Phys. Rev.* **D 78** (2008) 013004 [arXiv:0802.0007] [SPIRES].

[34] A.D. Martin, W.J. Stirling, R.S. Thorne and G. Watt, *Parton distributions for the LHC*, *Eur. Phys. J.* **C 63** (2009) 189 [arXiv:0901.0002] [SPIRES].

[35] M. Cacciari, M. Greco and P. Nason, *The p_T spectrum in heavy-flavour hadroproduction*, *JHEP* **05** (1998) 007 [hep-ph/9803400] [SPIRES].

[36] J.M. Campbell and R.K. Ellis, *An update on vector boson pair production at hadron colliders*, *Phys. Rev.* **D 60** (1999) 113006 [hep-ph/9905386] [SPIRES].

[37] Tevatron Electroweak Working Group collaboration, *Combination of CDF and D0 results on the mass of the top quark*, arXiv:0903.2503 [SPIRES].

[38] Z. Sullivan, *Understanding single-top-quark production and jets at hadron colliders*, *Phys. Rev.* **D 70** (2004) 114012 [hep-ph/0408049] [SPIRES].

[39] ALEPH, DELPHI, L3, OPAL, SLD, LEP Working Group, SLD Electroweak group and Heavy Flavor groups collaboration, *Precision electroweak measurements on the Z resonance*, *Phys. Rept.* **427** (2006) 257 [hep-ex/0509008] [SPIRES].

JHEP10(2009)042